Search for azimuthal anisotropic flow in proton–proton collisions

Bachelor Thesis
by
Adam Johansson

Supervisor:
Peter Christiansen

Division of Particle Physics
May 2015

Abstract

In high energy heavy ion collisions a new state of matter called quark gluon plasma is produced. An important observable is azimuthal anisotropy flow. Data from the ALICE experiment is used in the search for azimuthal anisotropic flow in pp collisions, at $\sqrt{s_{NN}} = 7$ TeV. p–Pb collisions at $\sqrt{s_{NN}} = 5.02$ TeV are used to create a baseline. It is expected to find symmetries in $\Delta\eta$ and $\Delta\varphi$ for a mini-jet. Results are obtained using a simplified two–particles correlation method together with a simplified Bethe–Bloch particle identification (PID) in two trigger ranges, $p_{\mathrm{T}}^{trig} > 2$ GeV/c and $p_{\mathrm{T}}^{trig} > 3$ GeV/c. The analysis is performed using the ALICE Time Projection Chamber. The results are compared to Monte Carlo simulations from the event generator PYTHIA.

Populärvetenskaplig sammanfattning

Kvark-Gluon-Plasma (QGP) är ett tillstånd av materia som har väldigt hög densitet och en temperatur på 2,000,000,000,000 K. Man tror att universum såg ut såhär precis efter the Big Bang, *Den Stora Smällen*. Vid detta tillstånd kunde inte hadroner (t.ex. protoner och neutroner) bilda atomkärnor som är grunden till all materia. Detta inträffar på grund av att gluonerna, som binder ihop kvarkarna inuti hadronerna, blir svagare på korta avstånd. Istället rörde sig kvarkar och gluoner fritt. Men när universum svalnar så började gluonerna binda ihop kvarkar till hadroner.

Man kan skapa kvark-gluon plasma genom att accelerera kärnor till nära ljusets hastighet och låta dem kollidera med varandra. Plasman existerar endast under en kort period innan det kyls ner och hadroner bildas. Man har sett att plasman beter sig som en perfekt vätska med väldigt låg viskositet.

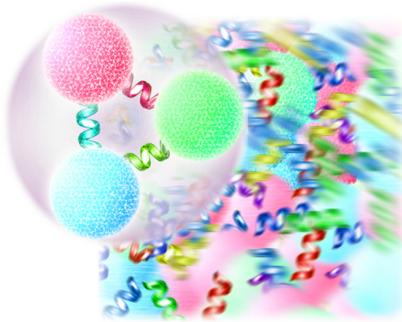

Figure 1: En hadron av tre kvarkar ihopbudna av gluoner. Vid väldigt höga temperaturer orkar inte gluonerna hålla ihop kvarkarna och kvark-gluon-plasma bildas [1]

Partikelfysiken studerar elementarpartiklar och deras växelverkan mellan varandra. Genom att kollidera partiklar vid väldigt höga energier kan skapa QGP. För att nå dessa höga energier krävs det kraftfulla maskiner, så kallade partikelacceleratorer. Det finns flera acceleratorer runt om i världen men världens största, the Large Hadron Collider (LHC), ligger vid CERN utanför Geneve i Schweiz. Där kolliderar man protoner och blykärnor för att studera vad som händer, vad för partiklar som skapas och hur de interagerar de med varandra.

Genom att mäta dessa partiklar som bildas i nedkylningen kan man ta reda på mer om QGPs egenskaper. Man har mycket kunskap om hur den fungerar vid bly–kollisioner och proton–bly–kollisioner. Därför ligger fokus i denna uppsats på att hitta bevis för plasman i proton–kollisioner. Analysen utförs genom en förenklad två–partikel-korrelation, där man mäter vinkelavståndet mellan två partikelspår, tillsammans med en partikelidentifiering (PID). Förhoppningsvis ska detta leda till mer förståelse om QGP.

Acknowledgements

First of I would like to thank my supervisor Peter Christiansen for giving me this opportunity. I thank him for all the help and support during this time. A thank you to David Silvermyr who gave insightful tips with the thesis and programming.

I would also like to thank Madeleine Peterson Sjögren, Martin Ljunggren, Tuva Richert, and Vytautas Vislavičius for all the help with the physics, and also all the fun things that we did outside the office.

And to my parents. I know you have tried to understand what I am doing with my life. Here is a small part of it.

Contents

Introduction

In this thesis the search for azimuthal anisotropic flow is performed using data from the ALICE experiment. ALICE is one of the experiments at the Large Hadron Collider (LHC), at CERN near Geneva, Switzerland. ALICE is focusing on strongly interacting particles at high energy densities. It has been observed that for Pb–Pb (lead–lead) and p–Pb (proton–lead) collisions a new state of matter, called Quark Gluon Plasma (QGP), is produced. In the QGP quarks and gluons are not bound together inside a hadron, which allows studies of the strong force. A good way to describe the produced state is by hydrodynamical models, as the QGP has been found to behave as a perfect liquid [2]. This is where the term "flow" comes in, as particle flow is a way of describing how the collided nuclei behave right after the collision.

It is of great interest to see if the QGP can be created in small systems, but it is hard to observe as the created state will be both very small and short-lived. The analysis starts with creating a baseline with p-Pb collisions for low and high multiplicity events at $\sqrt{s_{NN}} = 5.02$ TeV. The method used is a simplified version of the two-particle correlation together with particle identification (PID). Thereafter the analysis is performed for minimum bias (all events with no bias from restricted trigger conditions) pp collisions, at $\sqrt{s_{pp}} = 7$ TeV, using the same method as with p–Pb collisions. Lastly, an event generator called PYTHIA [3] is used to compare with the data.

The thesis will begin by giving some background theory of the elementary particles, how they interact and what effects that can lead to, in section 1 and section 2. Thereafter a description of the accelerator and the detector used in the ALICE experiment will be given in section 3. In the next section the analysis methods are described, and the result and conclusion are presented in the two following sections, 5 and 6.

1 Theory

1.1 The Standard Model

Particle physics is the study of the elementary particles in nature, and the forces acting between them. The Standard Model (SM) is the theory that attempts to explain the properties and interactions of all known elementary particles and forces that can be created in laboratories. In Fig. 2 all known particles are presented. There are two half-integer spin groups of fermions called leptons and quarks, and one integer spin group of gauge bosons. The fermions are divided into three generations according to their mass. The six leptons are: electron, electron neutrino; muon, muon neutrino; tau, tau neutrino. The leptons, except for the neutrinos, carry electric charge. There are also six quarks known as: up, down; charm, strange; top, bottom. The quarks carry both electric and colour charge. The elementary particles have anti-particles, which have the same mass but opposite charge.

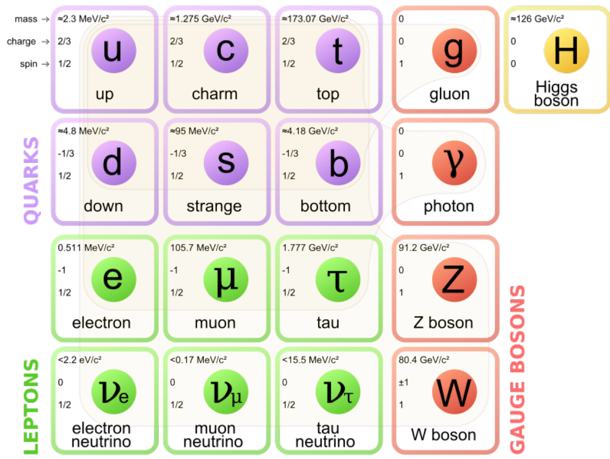

Figure 2: The elementary particles of the Standard Model[4]. The three generations of leptons and quarks are presented in the first three columns. The gauge bosons are in the fourth, and the Higgs boson is alone in the fifth column.

The gauge bosons are responsible for three out of four interactions between the fermions. The forth force, gravity, has not yet been explained on a microscopic level. Gluons are the strong force mediators. They mediate the interaction between particles carrying colour charge, i.e. gluons and quarks. The Z^0 and $W^{+/-}$ bosons are mediators of the weak force which interacts with all left-handed fermions. The electromagnetic interaction is described by Quantum Electrodynamics (QED). The mediators in electromagnetic interactions are photons which interacts with all particles carrying electric charge. The last particle is the Higgs boson, a neutral spin-0 particle associated with the Higgs field [5].

1.2 Quantum Chromodynamics

Quantum Chromodynamics (QCD) is the theory describing the strong force in the Standard Model. The force mediators are gluons which couple to colour charge similar to how photons couple to electric charge. The quarks carry colour charge that can be either red, green or blue (anti-red, anti-green or anti-blue for anti-particles). Gluons themselves carry colour charge, a colour and an anti-colour, allowing them to self-interact. Gluons can therefore emit and absorb new gluon pairs, leading to an anti-screening of the original charge, i.e. an increase of the force at large distance. Because of this there are two limits of the strong force: confinement, at large distances, and asymptotic freedom, at short distances.

Confinement requires that no free colour charged particles can be observed but instead are bound inside colour neutral hadrons. Asymptotic freedom means that the strong force gets weaker at distances below ≈ 0.1 fm. Quarks act as if they were free inside hadrons. The potential between two quarks changes over distances. These limits are characterized by the *running coupling constant*, α_s, which is ~ 1 for confinement and $<< 1$ for asymptotic freedom.

Hadrons consist of quarks and gluons, called partons. Mesons have two quarks and baryons have three, which are combined into colour neutral states. These quarks are called the valence quarks and carry the largest fraction of the hadron momentum. There are also sea quarks, gluons and virtual quark-antiquark pairs carrying a smaller fraction of the hadron momentum [5].

1.3 Quark Gluon Plasma

The Quark Gluon Plasma (QGP) is a state of matter at high energy densities where quarks and gluons are deconfined. At high density a quark will not be able to identify its partners inside a hadron. This allows quarks and gluons to move freely around inside a volume much larger than a hadron. Therefore, by studying the QGP the strong force can be studied at the quark level.

Studying the QGP can also provide more information about the evolution of the Universe. It is suggested that a few microseconds after the Big Bang the Universe was in the QGP state, too hot and dense to form hadrons. It is this state that is recreated in the laboratory by colliding heavy ions. Fig. 3 shows a phase diagram of the matter strongly interacting.

2 High Energy Collisions

2.1 Heavy Ion Collisions

Heavy Ion Collisions are a tool to study how nuclear matter behaves at high energies. Usually gold or lead nuclei are collided, as they are stable and consist of many nucleons. The nuclei are Lorentz contracted (see Fig. 4), due to relativistic effects, and collide with an impact parameter **b**, where the impact parameter is the transverse distance between

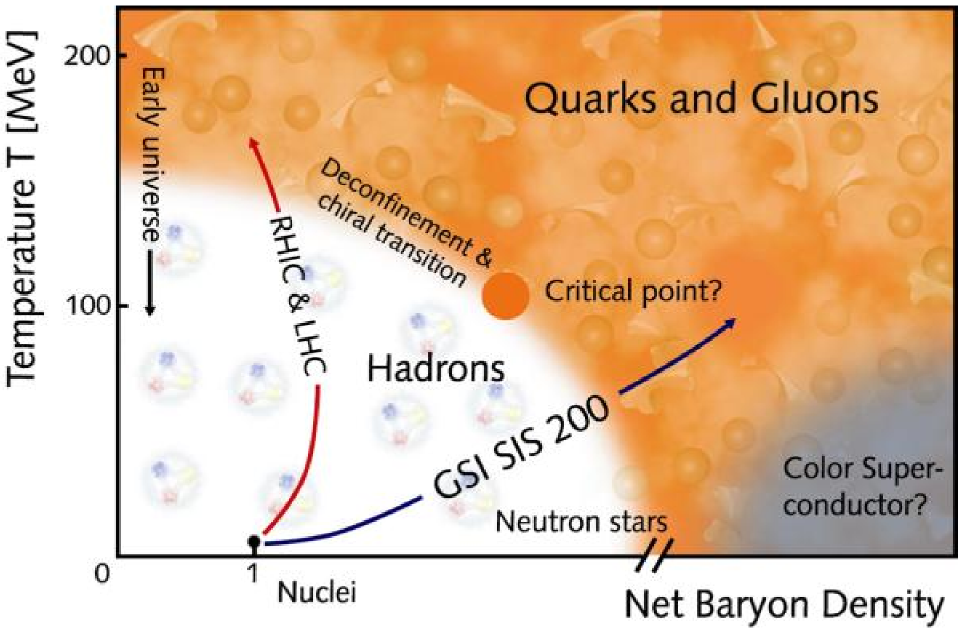

Figure 3: Phase diagram of matter in Temperature-Baryon Density plane. The two distinct phases of normal hadronic matter and QGP are indicated [6].

the centres of the two nuclei. The smaller **b** is, the greater the number of participating nucleons. The nucleons in this overlapping region interact with each other creating a high density *fireball*. This *fireball* expands and cools, until it reaches the *freeze out temperature*, at around 170 MeV [2], where the quarks and gluons hadronize. These final hadrons are detected by the experiment and are used to infer properties of the QGP. Research of this type of collisions have been performed at several different research facilities such as the LHC at CERN and the RHIC at Brookhaven National Laboratory.

When the two nuclei collide the partons can interact differently, depending on how much momentum they are exchanging. The partons exchanging a small amount of the momentum also exchange colour, giving rise to strong colour fields that can produce new quark-antiquark pairs. These soft collisions form the bulk matter, i.e. the QGP.

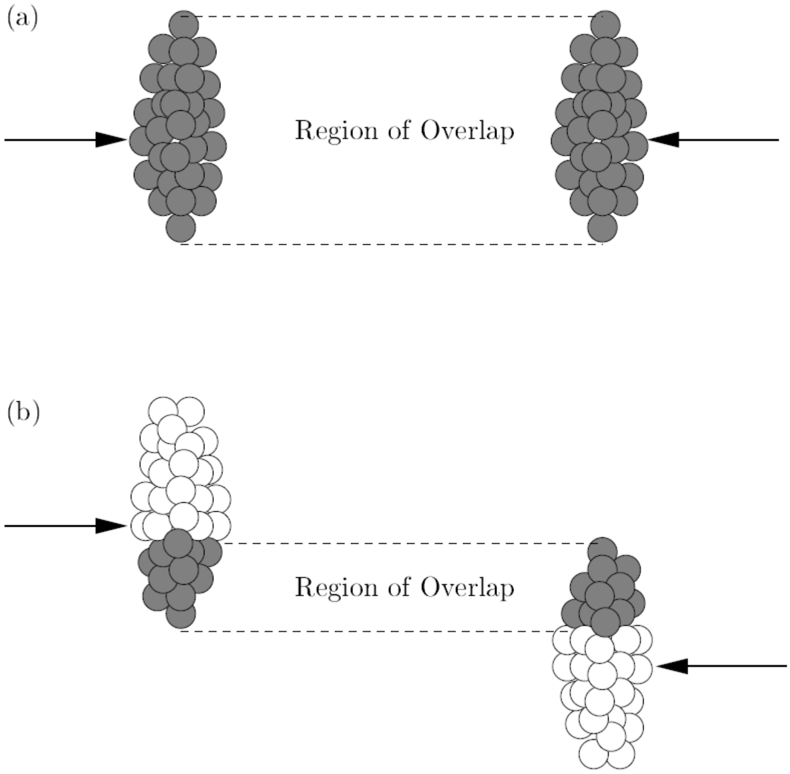

Figure 4: A representation of a central (a) and a peripheral collision (b). Central collisions have many nucleons participating and a high multiplicity of produced particles, while peripheral collisions have few nucleons participating and a low multiplicity of produced particles [7].

The partons can also scatter in hard collisions, where in addition to colour exchange, there is a large momentum transfer. The partons are kicked out and hadronize, producing jets. To conserve momentum, two jets of opposite direction are produced. If one parton traverses the QGP it will lose energy via gluon radiation, or elastic scattering.

2.2 Heavy ion physics observables

2.2.1 Transverse momentum

In ALICE the longitudinal z-direction has been defined along the beam axis, x is horizontal and y is vertical. The fraction of momentum carried by a particle perpendicular to the beam axis is called the *transverse momentum*, p_{T} . It is interesting to look at p_{T} as it is produced in the collision. p_{T} is defined as

$$p_{\mathrm{T}} = \sqrt{p_x^2 + p_y^2} \tag{1}$$

2.2.2 Rapidity and Pseudorapidity

Rapidity is a smart way to characterize longitudinal momentum in the beam-direction. Rapidity is defined as

$$y = \frac{1}{2} \ln \left(\frac{E + p_z}{E - p_z} \right) \tag{2}$$

where E is the energy of the particle and p_z is the momentum in the z-direction. Rapidity is additive for Lorentz boosts along the beam-axis. If the p_{T} carried by a particle is much larger than its mass, the rapidity can be approximated with pseudorapidity. Pseudorapidity is related to the angle the particle has relative to the beam axis. It is defined by

$$\eta = \frac{1}{2} \ln \left(\frac{|\mathbf{p}| + p_z}{|\mathbf{p}| - p_z} \right) = -\ln \left(\tan \frac{\theta}{2} \right) \tag{3}$$

where θ is the angle relative to the beam axis. Pseudorapidity is boost invariant as it is a measure orthogonal to the beam-axis. Pseudorapidity is often a more useful observable, especially in the absence of particle ID for the detected particle [8].

2.2.3 Anisotropic Azimuthal Flow

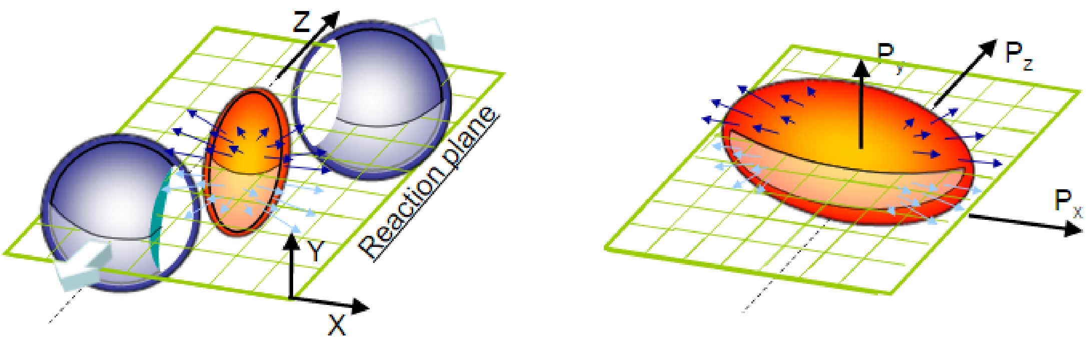

Figure 5: Schematic view illustrating the reaction plane and the almond shape in a peripheral collision which converts into a final momentum-space anisotropy [9].

The QGP is observed to behave as a perfect liquid that can be described by nearly ideal hydrodynamical models [2]. The term *flow* enters as the QGP has the collective behaviour of a liquid. In a heavy ion collision the reaction plane is defined as the plane containing the momenta of the beams and the impact parameter **b**. A non-central collision produces an initial anisotropic, almond-shaped region. The energy density gradient converts this initial state spatial asymmetry into a final momentum-space anisotropy, which leads to anisotropic flow (see Fig. 5). It is therefore interesting to measure flow, as it probes the initial state right after the collision. The observed azimuthal anisotropy can be expressed as a Fourier expansion

$$\frac{dN}{d\eta d^2 p_\mathrm{T}}(\varphi) = \frac{dN}{2\pi p_\mathrm{T} dp_\mathrm{T} d\eta}[1 + \sum_{n=1}^{\infty} 2v_n \cos k(\varphi - \psi_n)] \tag{4}$$

where η is the pseudorapidity and φ is the azimuthal angle of the particles. v_n is the n-th Fourier coefficient (called harmonic or anisotropy parameter) and ψ_n is the n-th order symmetry plane. Each harmonic correspond to the shape of the flow. The v_1, v_2, and v_3 correspond to directed, elliptic, and triangular flow. There are even higher order coefficients corresponding to other types of flow, but they are small, and not studied here. From Eq. 4 the flow coefficients can be found [10]

$$v_n = \langle \cos[n(\varphi - \psi_n)] \rangle \tag{5}$$

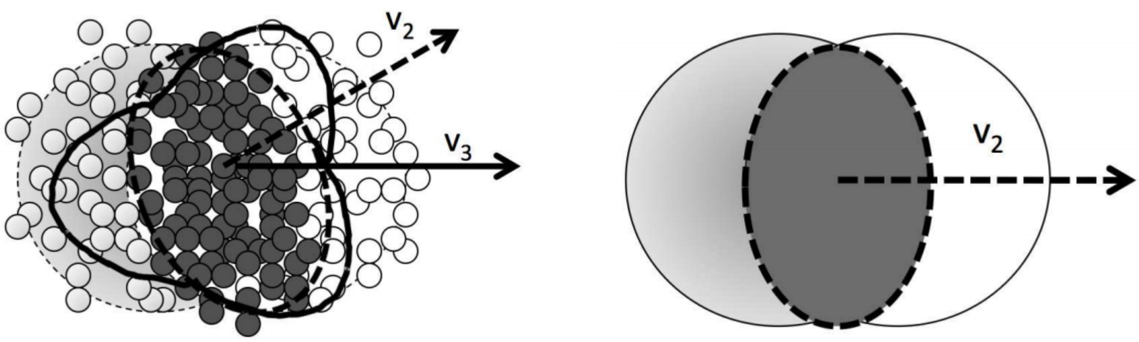

Figure 6: Left: Elliptic and triangular flows. Right: Elliptic flow from the almond shape initial state produced from the overlapping region in a collision [11].

2.3 QGP in small systems

It has been observed in high energy collisions that produced particles form a ridge-like structure. A way of studying this is to use two-particle correlation, which correlates the particle with highest momentum, p_T^{trig}, with associated particles, p_T^{asso}, that lie inside the same transverse momentum interval for that event. The two-particle correlation method measures the azimuthal difference $\Delta\varphi$ and pseudorapidity difference $\Delta\eta$. The correlation is established as the associated per-trigger-yield for different intervals of p_T^{trig} and p_T^{asso}. The associated per-trigger yield is measured as

$$\frac{1}{N_{trig}} \frac{d^2 N_{asso}}{d\Delta\eta d\Delta\varphi} = \frac{S(\Delta\eta, \Delta\varphi)}{B(\Delta\eta, \Delta\varphi)} \tag{6}$$

where $S(\Delta\eta, \Delta\varphi)$ is the signal distribution for particle pairs in the same event of the associated yield per trigger, and $B(\Delta\eta, \Delta\varphi)$ is the background distribution, calculated with event mixing, which corrects for pair acceptance and pair efficiency. Event mixing pairs an event's trigger particle to associated particles from many other events [12, 13].

2.3.1 Double ridge structure

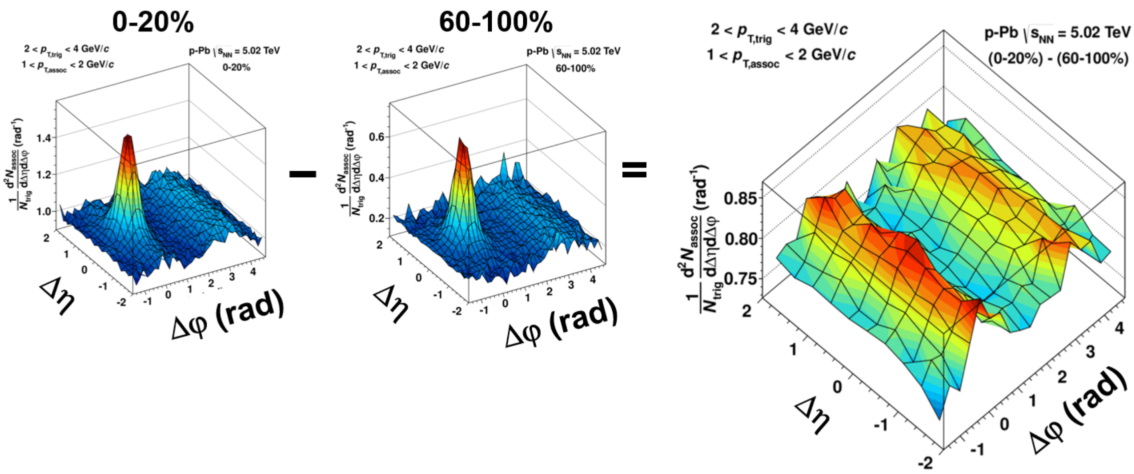

Figure 7: A subtraction of low multiplicity events from high multiplicity events shows a double ridge structure. This is from p–Pb collision at $\sqrt{s_{NN}} = 5.02$ TeV at ALICE [14].

The ridge structure is produced by the excess particles in the collision along the beam and boosted by transverse flow. This structure is observed in high energy collisions and can best be described by anisotropic flow of particles emitted from an expanding system. The harmonics v_n can be expressed as

$$\frac{dN}{d\Delta\eta \, d\Delta\varphi} \propto 1 + \sum_{n=1}^{\infty} v_n^{trig} v_n^{asso} \cos(n\Delta\varphi) \tag{7}$$

where v_n^{trig} and v_n^{asso} are related to the associated per-trigger-yield particle correlation. By looking at the emitted particles one can obtain the mass dependence of v_2 by taking the correlation between a trigger hadron and an identified proton, pion or kaon.

In high multiplicity pp collisions there is an increase of pairs at $\Delta\varphi = 0$, leading to a ridge structure at the near side [15]. Central p–Pb collisions show a double ridge structure, consistent with Pb–Pb collisions. In order to reveal this structure, two–particle correlations for high and low multiplicity events are calculated separately. Both of these are dominated by jets at around $\Delta\varphi = \Delta\eta = 0$, which can be removed by subtracting the low multiplicity from the high multiplicity correlation, see Fig. 7. This subtraction of low multiplicity reveals a symmetrical double ridge, around $\Delta\varphi = 0$ and π, opposite in azimuthal angle, to the near-side ridge [14, 16].

2.3.2 Proton–Proton Collisions

This thesis is focusing on proton–proton (pp) collisions. The reason pp collisions are of interest, is to see if the energy density of matter is high enough also there to form a double ridge, as seen in p–Pb collisions, and if the volume is an important parameter.

3 Experiment

In this thesis data from the ALICE detector at CERN is analysed. This chapter briefly presents the facilities at CERN used to conduct heavy ion/proton-proton collisions.

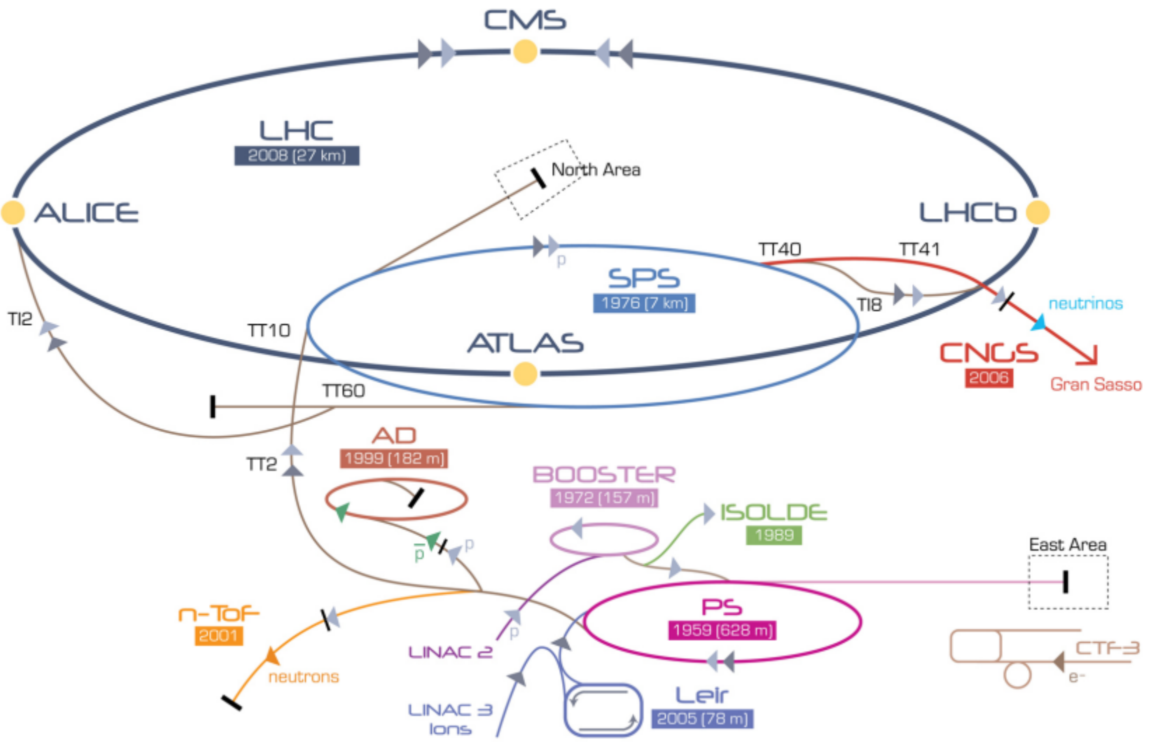

Figure 8: The LHC ring with its pre-accelerators[17]. The ALICE detector is situated at point 2 (left) in the LHC ring.

3.1 The Large Hadron Collider

The Large Hadron Collider (LHC) is the largest and most powerful particle accelerator in the world. It has a circumference of 27 km and consists of superconducting magnets and accelerating structures to boost the energy of the particles. The accelerator is built to collide protons and heavy ions. A number of pre-accelerators are used before injecting particles into LHC. Fig. 8 shows a schematic view of the LHC and its pre-accelerators.

The particles entering the circular accelerator are focused by magnetic fields. The beam momentum, p is limited by the maximal bending field B, and the radius $r$as

$$p = 0.3qBr \tag{8}$$

where q is the charge of the particle. For the first run of the LHC the obtained centre-of-mass energy per nucleon, $\sqrt{s}$, for proton–proton collisions (pp) is up to 8 TeV, proton–lead collision (p–Pb) is up to 5.02 TeV and lead–lead collision (Pb–Pb) is up to 2.76 TeV. For the second run of the LHC, starting now, the aim is to reach almost the double the centre-of-mass energy, with proton–proton collisions at 13 TeV.

There are six experiments at the LHC. The main experiments are ALICE, ATLAS, CMS and LHCb. The four different experiments are dedicated to explore certain fields of particle physics, such as heavy ion physics, super-symmetric particles and dark matter candidates.

3.2 ALICE

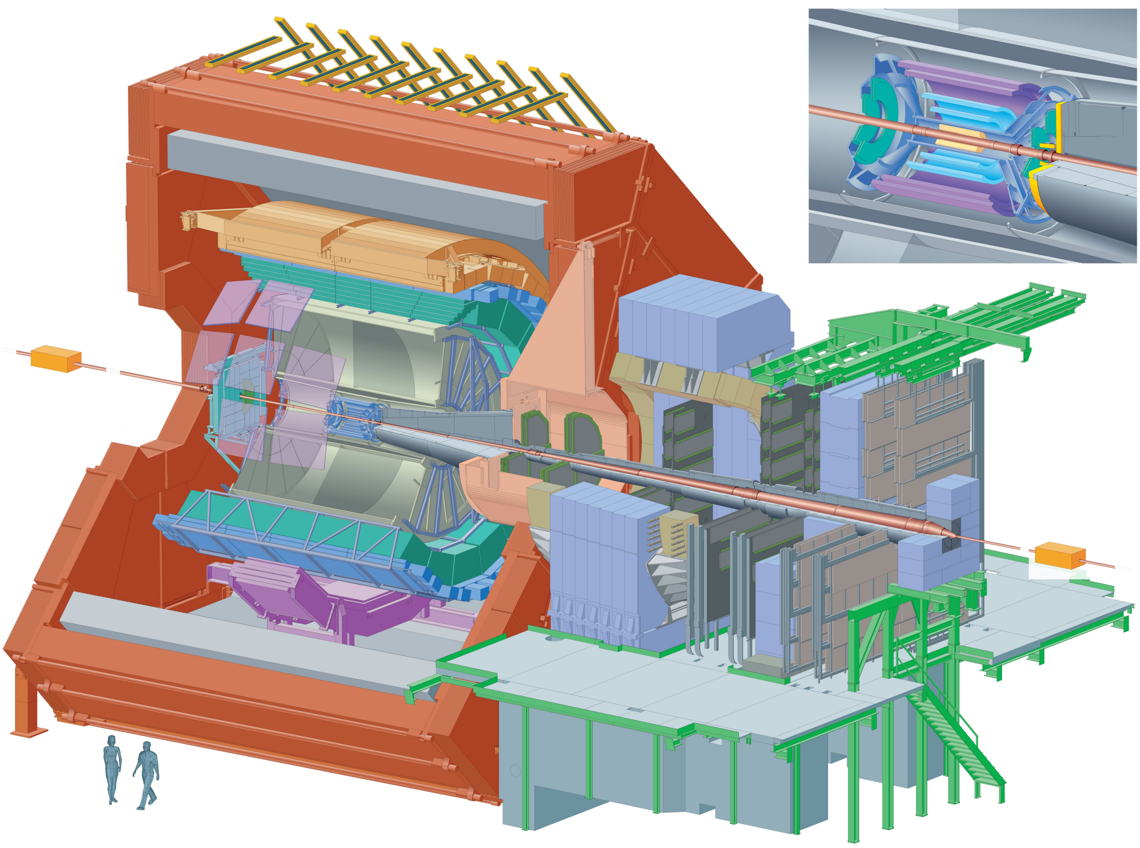

Figure 9: Schematic view of the ALICE detector [18].

ALICE (A Large Ion Collider Experiment) is the experiment at CERN specially designed to the study of heavy-ion collisions. ALICE consists of different types of detector systems, designed to detect and identify individual charged particles. The particle identification is done by measuring time-of-flight information, the Cherenkov radiation angle or the specific energy loss dE/dx and the momentum. In this thesis, the latter technique is used.

3.3 The Time Projection Chamber

The Time Projection Chamber (TPC) is the main tracking detector, in the central barrel of the ALICE detector. It covers the full azimuthal angle and pseudorapidity $|\eta| < 0.8$. It was designed to track charged particles in a single collision. The TPC is a hollow, gas filled cylinder with an inner radius of 0.8 m, an outer radius of 2.5 m, and 5 m long. Charged particles traversing the gas leave a track of electrons that drift towards the end plates. Multi-wire proportional chambers (MWPC) are situated at the end plates, to measure the charge in two dimensions. The z-coordinate is determined from the drift time. From this it is possible to determine the three-dimensional trajectory of the particle. By applying an external magnetic field over the detector one can determine the momentum from the curvature of the reconstructed track [19].

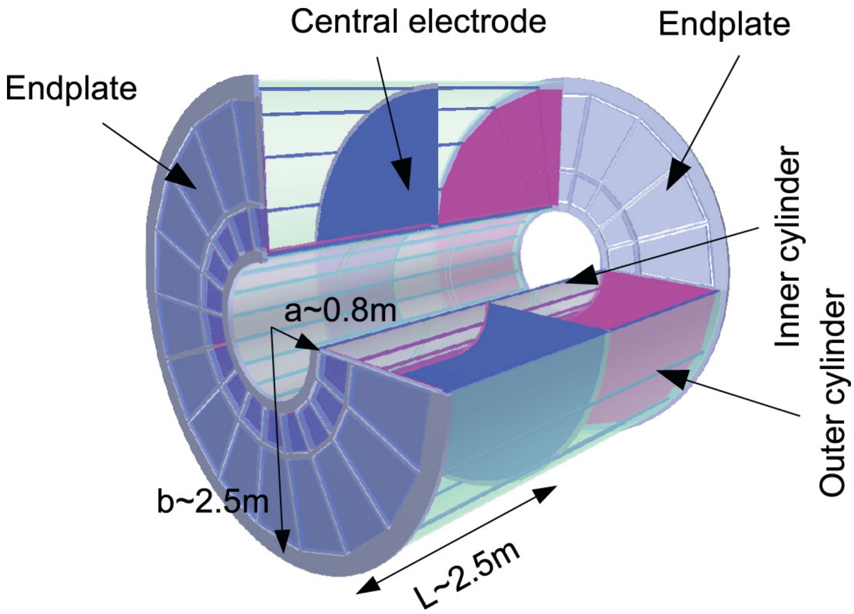

Figure 10: A schematic view of the ALICE TPC [20].

3.4 The specific energy loss dE/dx

When electrically charged particles move through a gas they lose their energy by ionization of atoms in the gas. This can be used to identify the particles in the TPC. The energy loss of a particle, travelling a distance x through a medium, can be described by the Bethe–Bloch formula

$$-\left\langle \frac{dE}{dx} \right\rangle = \frac{Dq^2 n_e}{\beta^2}\left[\frac{1}{2}\ln\frac{2m_e c^2\beta^2\gamma^2}{I^2} - \beta^2 - \frac{\delta(\gamma)}{2}\right] \tag{9}$$

where $D = \frac{4\pi\alpha^2 h^2}{m_e}$, m_e is the electron mass, q is the charge, $\beta = v/c$, $\gamma = \sqrt{1-\beta^2}$, n_e is the electron density, I is the mean ionization potential and δ is the dielectric screening correction. The energy loss initially decreases as the velocity increases because of the $1/\beta^2$ factor. For this thesis the energy loss is in this regime. The relation between β and the particle momentum, p, and energy, E, can be used in order to identify particles

$$\left\langle \frac{dE}{dx} \right\rangle \sim \frac{C}{\beta^2} \sim C\left(\frac{p^2+m^2}{p^2}\right) \tag{10}$$

where C is a scaling factor adjusted in the data and m is the rest mass of the particle one wants to identify.

4 Analysis Method

In p–Pb collisions the double ridge in $\Delta\eta$ at high multiplicity is observed, as mentioned in chapter 2. In this thesis the triggered two–particle correlation in $\Delta\eta$-$\Delta\varphi$ is measured for both low and high multiplicity events. The first goal is to create a simpler method using the p–Pb sample. This method will then be used to search for azimuthal anisotropic flow in pp collisions. It is expected to find symmetries in $\Delta\eta$ and $\Delta\varphi$ for a mini-jet. Mini-jets refer to jet-like processes that occur at lower momentum-scales. This analysis is therefore focusing at $\Delta\varphi \sim \pi/2$ where no jets are expected, and compare it to $\Delta\eta \sim \pi/2$. This will be compared to the pp collisions to see if there is a similar behaviour with p–Pb collisions.

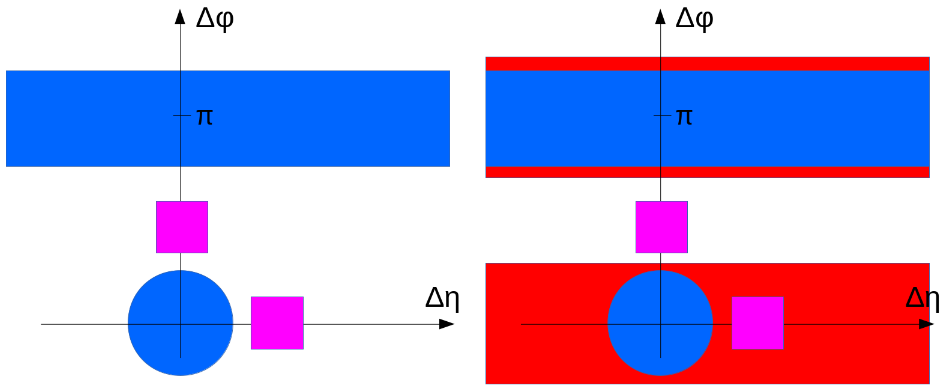

Figure 11: The pink boxes show the regions $\Delta\varphi \sim \pi/2$ (φ-gap) and $\Delta\eta \sim \pi/2$ (η-gap) where the analysis is focused. Left: Low multiplicity with no near ridge structure at $\varphi = 0$. Right: High multiplicity with a double ridge structure around $\varphi = 0$ and π

The method used is based on the two–particle correlation technique. The analysis is made in the programming language C++, using the data analysis framework ROOT [21].

A PYTHIA-simulation [3] of pp collisions at 7 TeV is also performed in order to better understand the result.

4.1 Simplified two–particle correlations

The aim of the method is to remove the non-collective components in order to obtain the double ridge structure. This thesis will use a simpler method of the two–particle correlation method from Eq. 6. A symmetry is expected for a mini-jet between $\Delta\varphi$ and $\Delta\eta$. Therefore, the analysis will only be looking at $\Delta\varphi \sim \pi/2$ and compare it to $\Delta\eta \sim 0.8$. This comparison is done because the full acceptance in the TPC of $|\eta|$ is < 0.8. In order to always have full acceptance, the trigger in η is required to be within $0.2 < |\eta| < 0.6$.

The first analysis of p–Pb collisions, at $\sqrt{s_{NN}} = 5.02$ TeV, looks at the charged particle ratio between η-gap and φ-gap against $p_{\rm T}$. The η-gap and the φ-gap are marked as pink boxes in Fig. 11. The expectation is that for low multiplicity the ratio between the particles in $\Delta\eta$ and $\Delta\varphi$ should be equal to 1. For high multiplicity the ratio should be above 1, as there is a boost of protons. This is not observed (see Fig. 12).

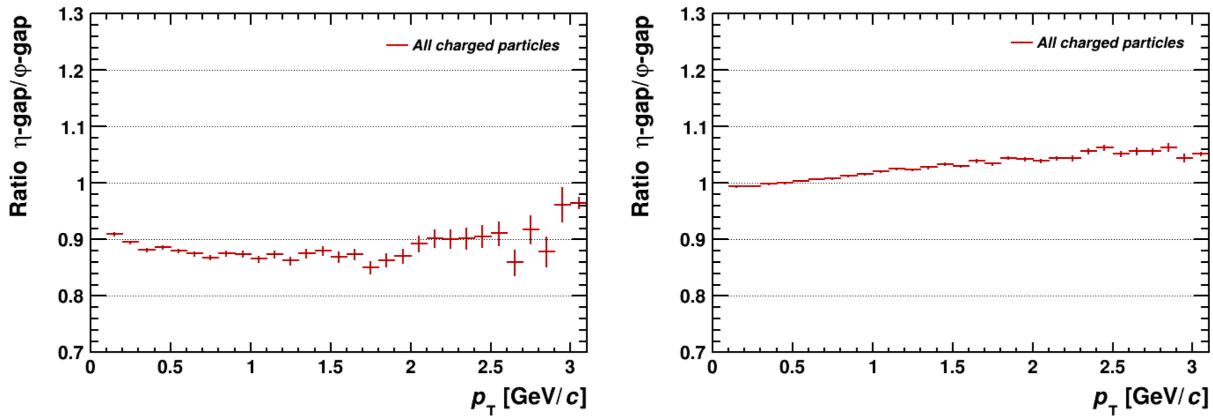

Figure 12: p–Pb collision at $\sqrt{s_{NN}} = 5.02$ TeV, $p_{\rm T}^{trig} > 2$ GeV/c using data from ALICE. The ratio is not following the expectation for ~ 1 for low multiplicity (left) and above 1 for high multiplicity (right).

In order to see if that is a correct assumption, a particle identification (PID) is performed. The PID is focusing on protons and pions, as it is observed that proton-to-pion ratio is enhanced, especially at high multiplicity (see Fig. 13). The PID uses the simplified Bethe–Bloch formula (Eq. 10), together with a cut in dE/dx (see Fig. 14, 15). Using this PID, the p–Pb data at $\sqrt{s_{NN}} = 5.02$ TeV is once more analysed to see if there is an efficiency problem.

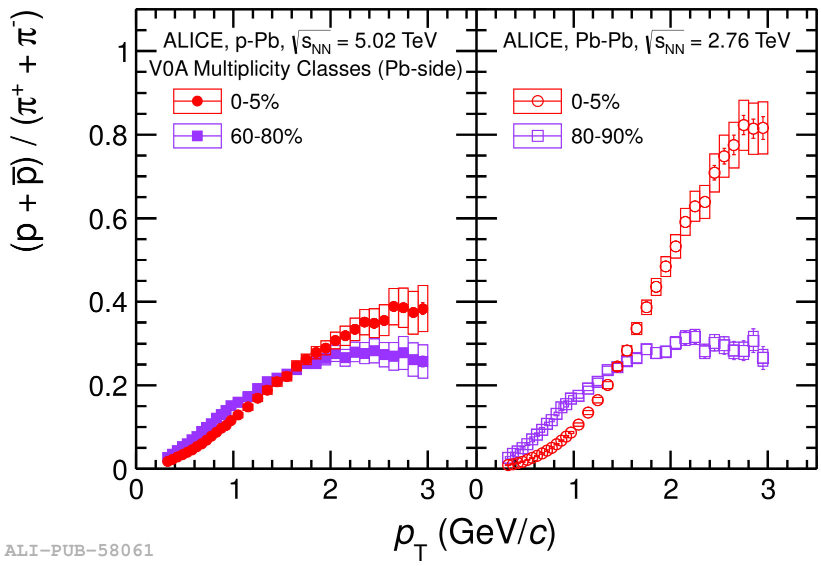

Figure 13: Proton-to-pion ratio as a function of p_{T} , measured at $\sqrt{s_{NN}}$ = 5.02 TeV for p–Pb collisions, and $\sqrt{s_{NN}}$ = 2.76 TeV for Pb–Pb collisions at ALICE[22].

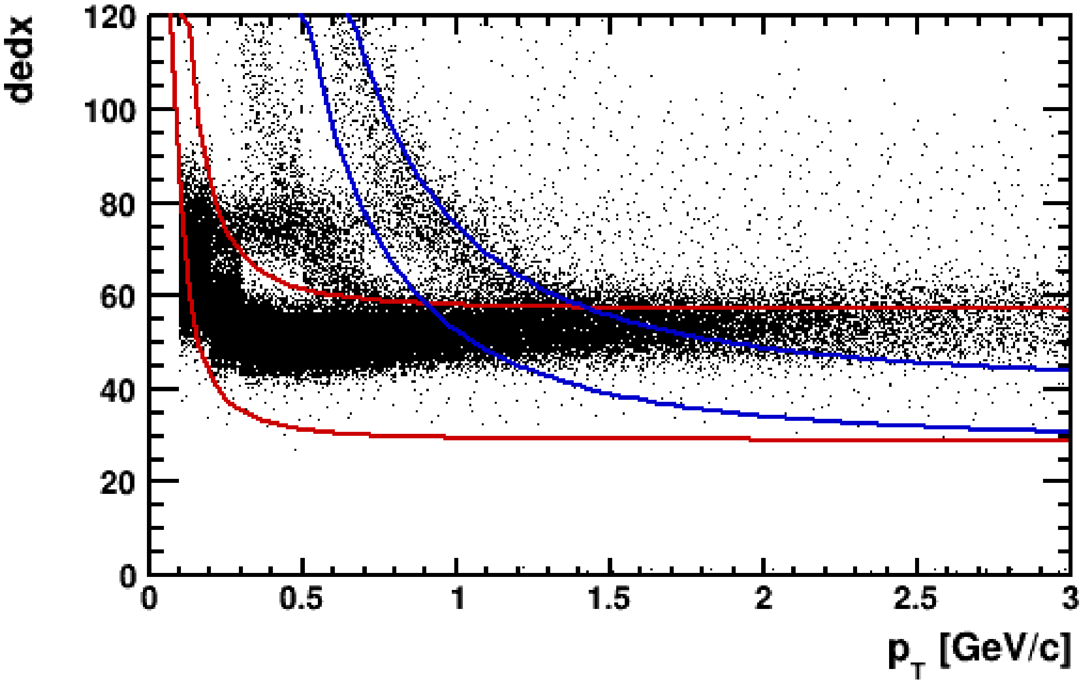

Figure 14: The simplified Bethe–Bloch formula (Eq. 10) plotted in order to separate pions (red lines) and protons (blue lines) from all other particles. The vertical structure seen at $dE/dx = 80$ is electrons and the vertical, banana-shape between the lines at around $p_{\mathrm{T}} = 0.5$ GeV/c are kaons.

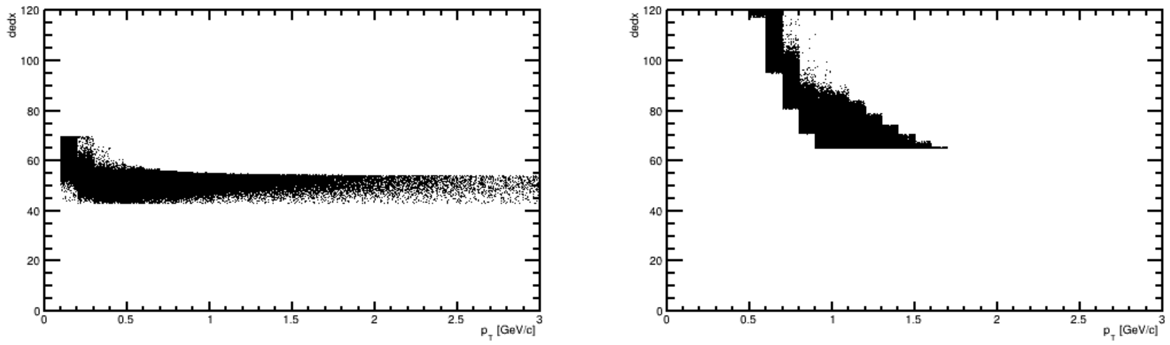

Figure 15: Left: The applied cut seen in Fig. 14 together with a dE/dx cut (Eq. 10), in order to extract pions. Right: The extracted protons

This new analysis shows that the ratio between the protons and pions have the same pattern as when looking at all charged particles which means that there is no problem with efficiency. The obtained results from p–Pb are used as a baseline for the analysis of the pp collisions.

The pp collisions considered are minimum bias events at $\sqrt{s_{pp}} = 7$ TeV, using the same simplified two-particle correlation method. It utilises the same PID for protons and pions. It is expected to have the same effects for pp collisions as in p–Pb collisions.
The last part of the analysis with data is to look at high multiplicity pp collisions. As there is no centrality cut in the data, it has to be done manually by creating a histogram over the number of tracks in the data. Thereafter, a cut is applied to get the 20% highest statistics giving the most central part of the collision, see Fig. 16.

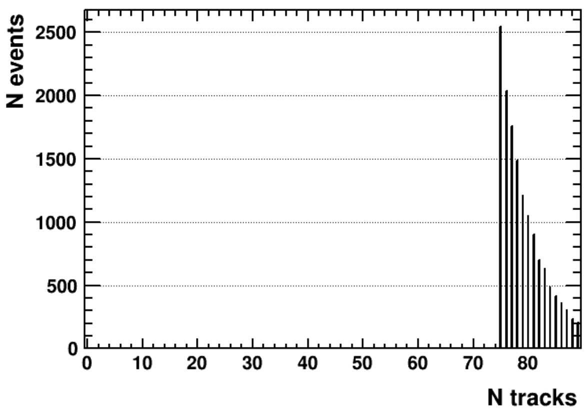

Figure 16: Histogram with number of events against number of tracks. A cut is applied in order to get the high multiplicity.

4.2 PYTHIA

Another part of this study is to use PYTHIA [3], a pp event generator program, in order to compare with the two–particle correlation result. PYTHIA is a program written in C++ for simulation of high-energy physics events. It generates events by the Monte Carlo method, with all features of a collision, such as hard processes, hadronisation and decays [3].

This simulated data is analysed with the same simplified two–particle correlation method as for the data. A small change is applied as it is possible to use both pseudorapidity and rapidity, because one can extract the generated particles, and obtain their respective mass. Another type of PID is used, as all particles are known by PYTHIA and therefore can be identified as protons and pions.

5 Results

In this section the results obtained from the analysis described in section 4 are presented. It is divided into two parts, where the first shows data for the created baseline from p–Pb collisions and the analysis of pp collisions. The second part shows the PYHTIA-simulation for both pseudorapidity and rapidity.

5.1 Data

The analysis using data was done in two different regions of p_{T} . The regions for the baseline, using p–Pb collisions, were $p_{\mathrm{T}}^{trig} > 2$ GeV/c and $p_{\mathrm{T}}^{trig} > 3$ GeV/c with both having cuts for high multiplicity at 0-20% and for low multiplicity at 60-100%. p–Pb collisions are shown in Fig. 17 and 18 for low multiplicity and high multiplicity events. This baseline is used as a reference to the pp collisions analysed at $p_{\mathrm{T}}^{trig} > 2$ GeV/c and $p_{\mathrm{T}}^{trig} > 3$ GeV/c. A cut is applied in order to extract the protons and pions from the data. This is used to compare protons and pions with all produced particles. For low multiplicity the behaviour was anticipated to be similar for protons and pions, but has been shown to have a lower ratio in $\Delta\eta/\Delta\varphi$. The expected boost of protons in $\Delta\eta$ in high multiplicity is not observed, as seen to the right of Fig. 17, 18, 19 and 20. It is more symmetrical in high multiplicity than in low multiplicity, opposite to what was expected.

The results from the data (Fig. 17, 18, 19, 20) show that the protons only go up to 1.5 GeV. The reason is associated with the fit curves presented in Fig. 14. As it can be seen, one cannot separate the protons from other particles at higher p_{T} . This cut was therefore done in order to get a clean proton sample. However, in the PYTHIA-simulation the protons are plotted up to 3 GeV as one does not have to separate them.

p–Pb results

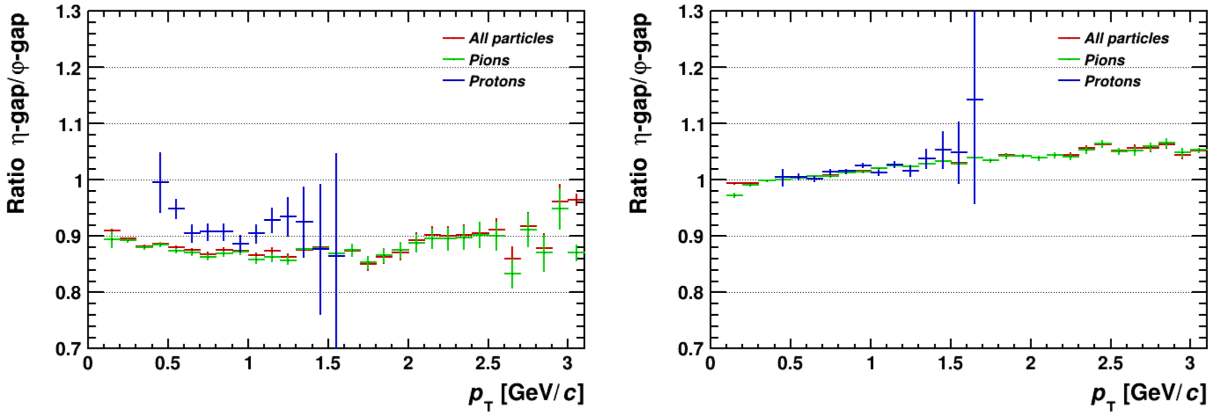

Figure 17: p–Pb collision at $\sqrt{s_{NN}} = 5.02$ TeV, $p_{\mathrm{T}}^{trig} > 2$ GeV/c, with low (left) and high (right) multiplicity, using data from ALICE.

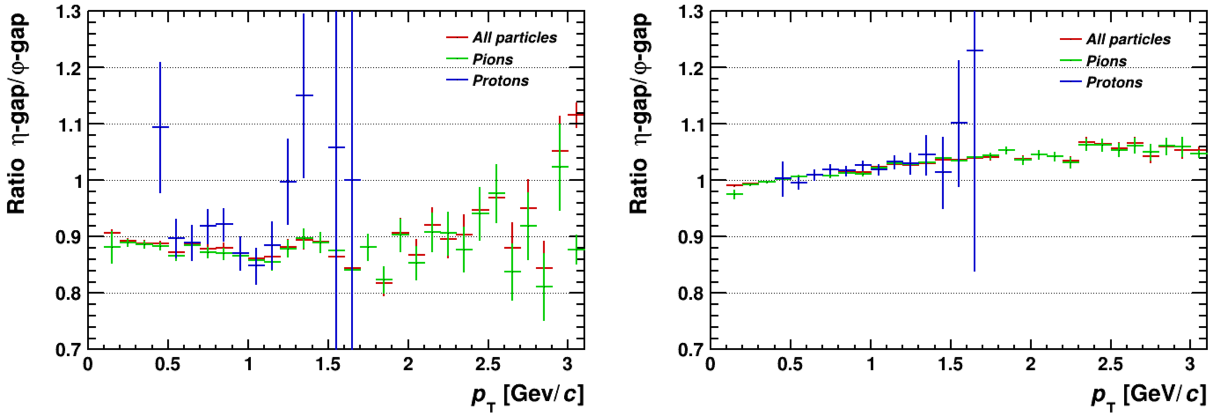

Figure 18: p–Pb collision at at $\sqrt{s_{NN}} = 5.02$ TeV, $p_{\mathrm{T}}^{trig} > 3$ GeV/c low (left) and high (right) multiplicity, using data from ALICE.

pp results

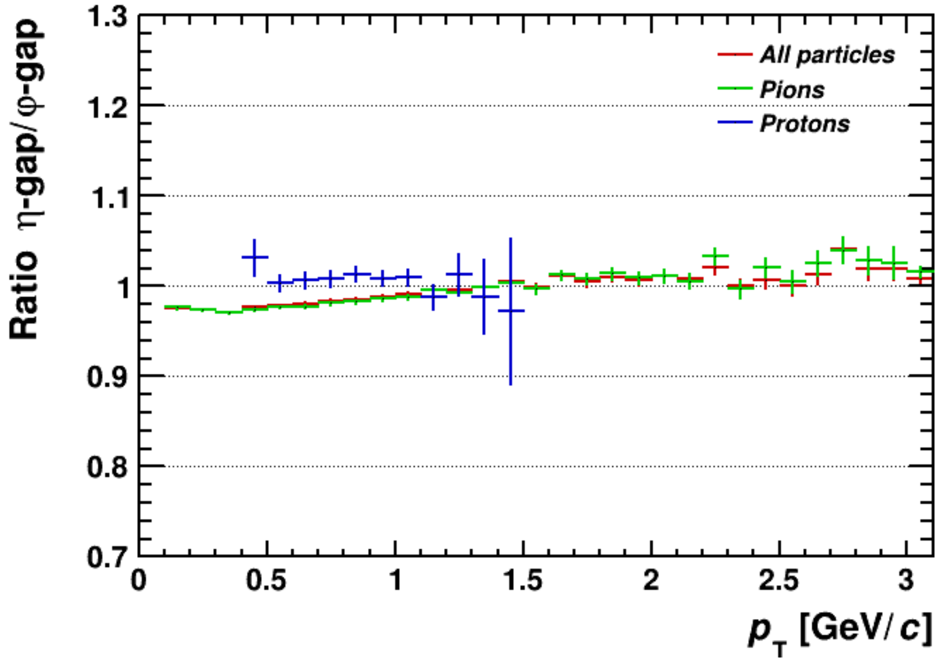

Figure 19: pp collisions at $\sqrt{s_{pp}} = 7$ TeV/c with $p_{\mathrm{T}}^{trig} > 2$ GeV/c using 79 million evemts.

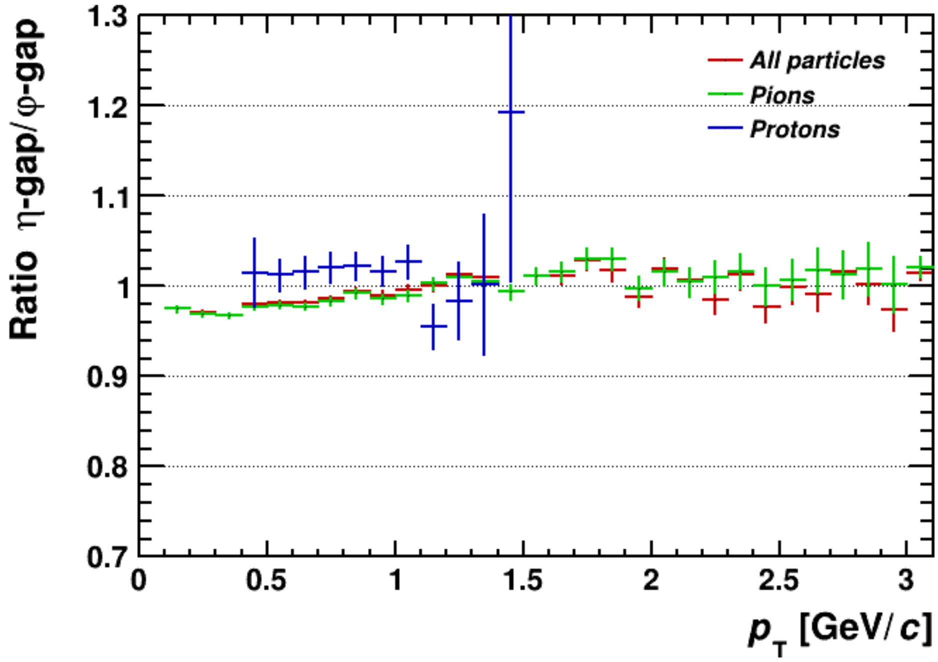

Figure 20: pp collisions at $\sqrt{s_{pp}} = 7$ TeV with $p_{\mathrm{T}}^{trig} > 3$ GeV/c, with 79 million events.

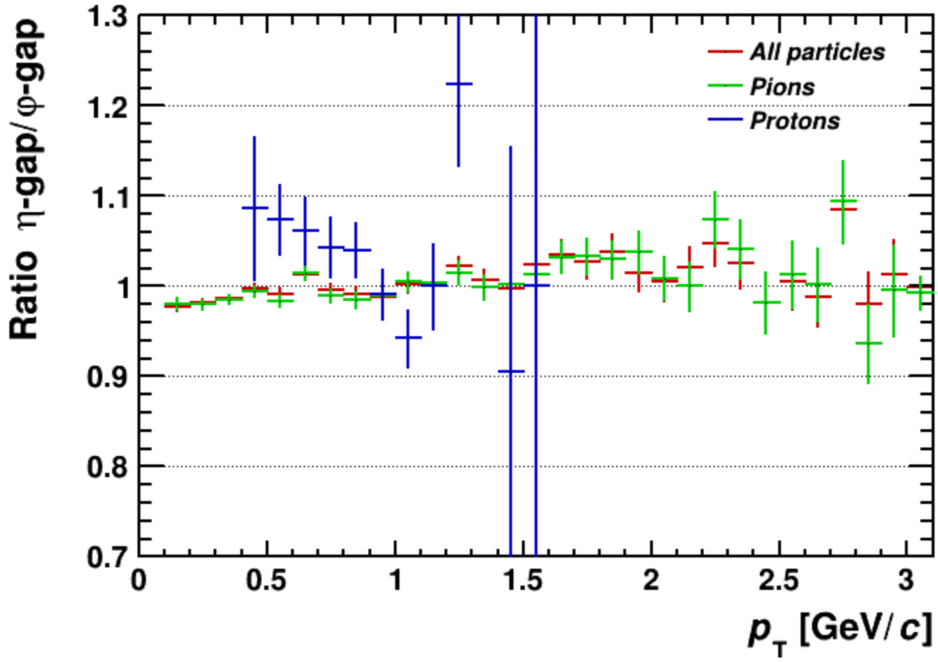

Figure 21: pp collisions at $\sqrt{s_{pp}} = 7$ TeV with $p_{\mathrm{T}}^{trig} > 2$ GeV/c, with 79 million events and 0-20% multiplicity

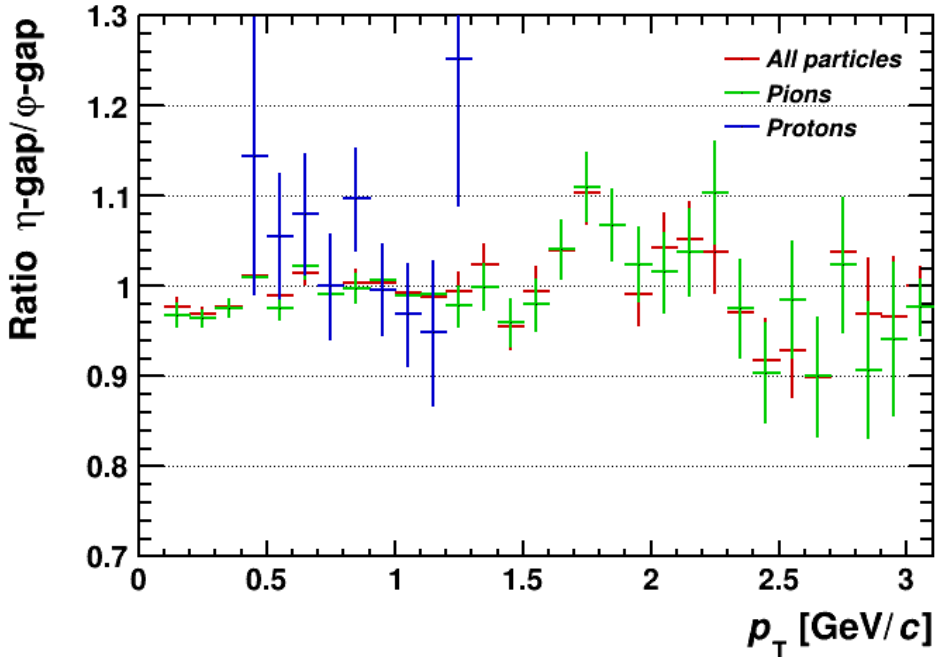

Figure 22: pp collisions at $\sqrt{s_{pp}} = 7$ TeV with $p_{\mathrm{T}}^{trig} > 3$ GeV/c, with 79 million events and 0-20% multiplicity

5.2 PYTHIA

The results from the PYTHIA-simulation are presented in Fig. 23 and 24. The results are from ∼33 million events, at 7 GeV, in the region $p_T^{trig} > 2$ GeV/c and $p_T^{trig} > 3$ GeV/c. The result is presented with the pseudorapidity to the left and the rapidity to the right.

PYTHIA results

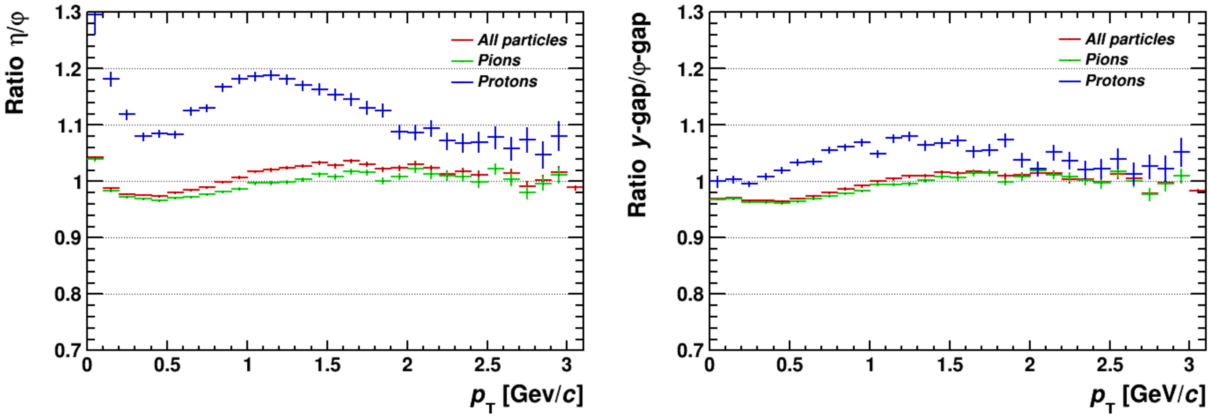

Figure 23: The ratio from 33 million PYTHIA generated at $\sqrt{s_{pp}} = 7$ TeV/c events with $p_T^{trig} > 2$ GeV/c. Left: The result when using pseudorapidity. Right: The result when using rapidity.

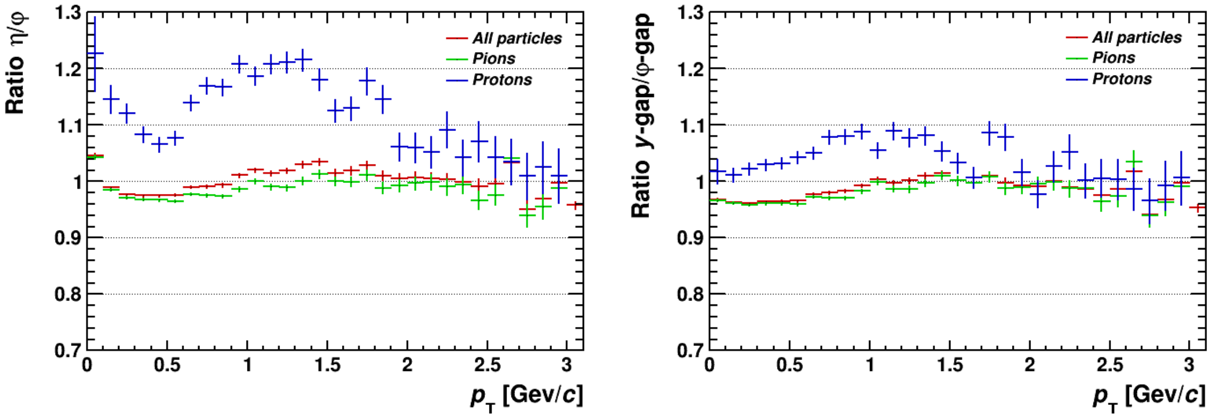

Figure 24: The ratio from 33 million PYTHIA generated at $\sqrt{s_{pp}} = 7$ TeV/c events with $p_T^{trig} > 3$ GeV/c. Left: The result when using pseudorapidity. Right: The result when using rapidity.

6 Conclusion

In this thesis, the search for azimuthal, anisotropic flow has been studied using a simpler method than the regular two particle correlation method. The idea was that one would observe that protons were pushed further out than pions in high multiplicity event and low multiplicity events would follow the symmetry in $\Delta\eta$ and $\Delta\varphi$ for a mini-jet.

After the first p–Pb analysis it was shown that the results did not follow these predictions. The first suggestion to why it did not follow the expectation was due to the efficiency in the experiment. That was discarded as the PID showed that both protons and pions followed the same pattern as when analysing all particles. It was observed that for low multiplicity the protons where pushed out instead at high multiplicity. This was opposite to the original idea.

The pp analysis used this baseline created from the p–Pb. What was observed then was that the protons followed the effect from p-Pb analysis of low multiplicity where protons were pushed out, instead of the anticipated effect of protons pushed out in high multiplicity. Why it is so remains unsolved.

There is good agreement between pp collisions and PYTHIA-simulations, especially when looking at rapidity. The ratio is around 1 and the protons are pushed out in similar way as for real data in pp collisions.

The anticipated effect of protons not being pushed out in high multiplicity events may have to do with the experiment is looking at a too low p_{T} -threshold. At $2 < p_{\mathrm{T}} < 8$ GeV/c there are more baryons forming than mesons, due to being energetically favoured. Even though the range $0 < p_{\mathrm{T}} < 3$ GeV/c shows significant increase in proton production (see. Fig. 13) this was not observed in the analysis where the cut for protons is applied at $p_{\mathrm{T}} < 1.5$ Gev/c.

Observing the last result in pp collisions with multiplicity (Fig. 22) there are som indication of the protons being pushed out. An analysis with a higher multiplicity could show even more clear effects of pushed out protons.

The cut applied in order to get a clean proton sample leads to many protons not being taken into account. In fact, looking at Fig. 14 one can observe that the protons merge together with the pions (and other particles) at ~ 1 GeV/c. Using the full, instead of a simplified version of, Bethe–Bloch could improve the PID result. All data used is from the TPC. ALICE has more specialized detectors for PID with better precision which could have been used to get a more precise result.

Bibliography

[1] http://i.livescience.com/images/i/000/017/486/i02/quark-gluon-plasma.jpg?1308851475.

[2] PHENIX Collaboration. Formation of dense partonic matter in relativstic nucleus–nucleus collisions at RHIC: Experimentalevaluation by the PHENIX collaboration. 2005.

[3] http://home.thep.lu.se/~torbjorn/pythia81html/pythia8100.pdf. Accessed: 2015-05-12.

[4] http://en.wikipedia.org/wiki/Standard_Model#/media/File:Standard_Model_of_Elementary_Particles.svg. Accessed: 2015-05-12.

[5] B.R. Martin and G.Shaw. *Particle Physics, 3rd Edition.* John Wiley and Sons Ltd, 2009.

[6] http://th.physik.uni-frankfurt.de/~scherer/vortrag/HHLR/figures_06/PhaseDiagram.jpg. Accessed: 2015-05-18.

[7] Stephen Andrew Bull. *Strange particle and antiparticle production in proton-beryllium interactions at 40 GeV/*c *at the CERN NA 57 experiment.* PhD thesis, University of Birmingham, 2005.

[8] Wojciech Florkowski. *Phenomenology of Ultra-Relativistic Heavy-Ion Collisions.* World Scientific Publishing Co. Pte. Ltd., 2010.

[9] http://www.quantumdiaries.org/wp-content/uploads/2011/02/FlowPr.jpg. Accessed: 2015-05-12.

[10] S. Voloshin and Y. Zhang. Flow study in relativistic nuclear collisions by Fourier expansion of Azimuthal particle distributions. 1996.

[11] http://inspirehep.net/record/1112008/files/arXiv:1204.4795.pdf?version=3.

[12] http://arxiv.org/pdf/1212.2001v3.pdf.

[13] Christian Bourjau. *Long-range angular correlations in soft and hard pPb collisions at a center-of-mass energy of 5.02 TeV measured with ALICE.* Master's thesis, Lund University, 2014.

[14] J.F. Grosse-Oetringhaus. *The double ridge phenomenon in p-Pb collisions measured with ALICE.* Presentation for the ALICE Collaboration, Moriond QCD 2013.

[15] Fu-Hu Liu, Tian Tian, and Ya-Qin Gao. On Two-Ridge Structure in Two-Particle Azimuthal Correlations in Proton-Lead Collisions at Large Hadron Collider Energy. *Adv.High Energy Phys.*, 2014, 2014.

[16] http://arxiv.org/pdf/1407.5808v3.pdf.

[17] http://upload.wikimedia.org/wikipedia/commons/thumb/7/72/CAC-acc_45.jpg/800px-CAC-acc_45.jpg. Accessed: 2015-05-12.

[18] http://aliceinfo.cern.ch/Public/Objects/Chapter2/ALICE-SetUp-NewSimple.jpg. Accessed: 2015-05-13.

[19] http://aliceinfo.cern.ch/TPC/node/7. Accessed: 2015-05-12.

[20] http://www.sciencedirect.com/science/article/pii/S0168900210030160. Accessed: 2015-05-12.

[21] https://root.cern.ch/.

[22] ALICE Collaboration. Multiplicity dependence of pion, kaon, proton and lambda production in p–Pb collisions at $\sqrt{s_{NN}} = 5.02TeV$. 2013.